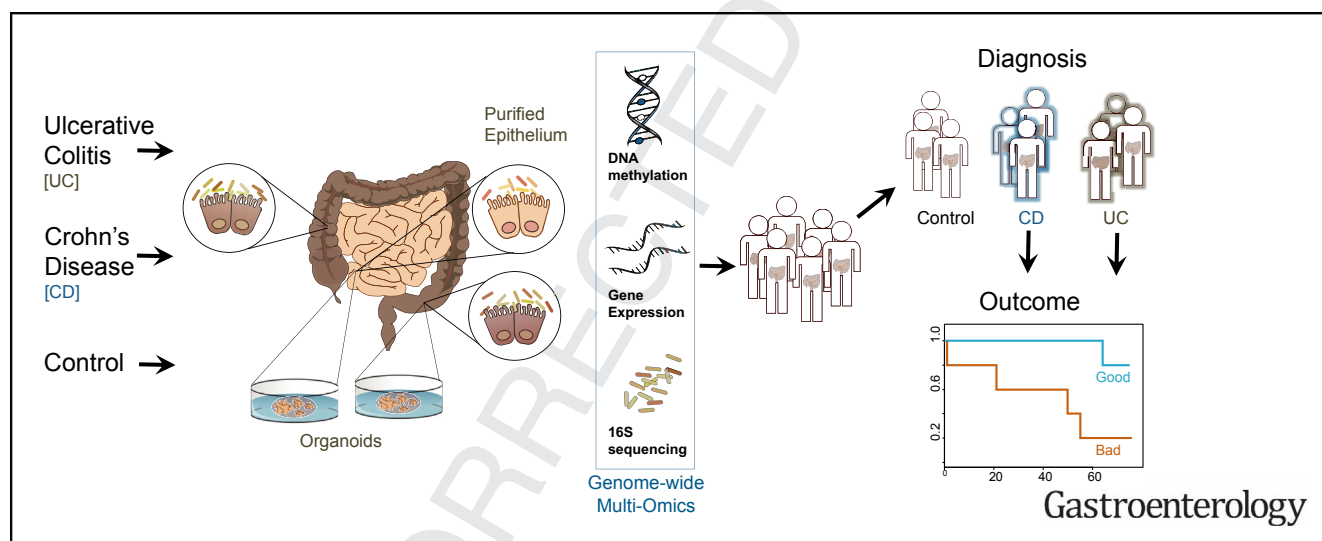


DNA Methylation and Transcription Patterns in Intestinal Epithelial Cells From Pediatric Patients With Inflammatory Bowel Diseases Differentiate Disease Subtypes and Associate With Outcome

Q17 **Kate Joanne Howell**,^{1,3,*} **Judith Kraiczky**,^{1,*} Komal M. Nayak,¹ Marco Gasparetto,^{1,2} Alexander Ross,^{1,4} Claire Lee,^{1,2} Tim N. Mak,¹ Bon-Kyoung Koo,⁴ Nitin Kumar,⁵ Trevor Lawley,⁵ Anupam Sinha,⁶ Philip Rosenstiel,⁶ Robert Heuschkel,² Oliver Stegle,^{3,§} and Q1 **Matthias Zilbauer**^{1,2,4,§}

¹University Department of Paediatrics, University of Cambridge, UK; ²Department of Paediatric Gastroenterology, University of Cambridge and Addenbrooke's Hospital, Cambridge, UK; ³European Molecular Biology Laboratory, European Bioinformatics Institute, Wellcome Genome Campus, Hinxton, Cambridge, UK; ⁴Wellcome Trust - Medical Research Council Stem Cell Institute, University of Cambridge, Cambridge, UK; ⁵Wellcome Trust Sanger Institute, Wellcome Trust Genome Campus, Hinxton, UK; ⁶Institute of Clinical Molecular Biology (IKMB), Kiel University, Kiel, Germany



BACKGROUND & AIMS: We analyzed DNA methylation patterns and transcriptomes of primary intestinal epithelial cells (IEC) of children newly diagnosed with inflammatory bowel diseases (IBD) to learn more about pathogenesis. **METHODS:** We obtained mucosal biopsies (n = 236) collected from terminal ileum and ascending and sigmoid colons of children (median age, 13 years) newly diagnosed with IBD (43 with Crohn's disease [CD], 23 with ulcerative colitis), and 30 children without IBD (controls). Patients were recruited and managed at a hospital in the United Kingdom from 2013 through 2016. We also obtained biopsies collected at later stages from a subset of patients. IECs were purified and analyzed for genome-wide DNA methylation patterns and gene expression profiles. Adjacent microbiota were isolated from biopsies and analyzed by 16S gene sequencing. We generated intestinal organoid cultures from a subset of samples and genome-wide DNA methylation analysis was performed. **RESULTS:** We found gut segment-specific differences in DNA methylation and

transcription profiles of IECs from children with IBD vs controls; some were independent of mucosal inflammation. Changes in gut microbiota between IBD and control groups were not as large and were difficult to assess because of large amounts of intra-individual variation. Only IECs from patients with CD had changes in DNA methylation and transcription patterns in terminal ileum epithelium, compared with controls. Colon epithelium from patients with CD and from patients with ulcerative colitis had distinct changes in DNA methylation and transcription patterns, compared with controls. In IECs from patients with IBD, changes in DNA methylation, compared with controls, were stable over time and were partially retained in ex-vivo organoid cultures. Statistical analyses of epithelial cell profiles allowed us to distinguish children with CD or ulcerative colitis from controls; profiles correlated with disease outcome parameters, such as the requirement for treatment with biologic agents. **CONCLUSIONS:** We identified specific changes in DNA methylation and transcriptome patterns in IECs from

EDITOR'S NOTES

BACKGROUND AND CONTEXT

The intestinal epithelium is thought to play a critical role in the pathogenesis of inflammatory bowel Diseases (IBD), yet evidence derived from primary human tissue remain scarce.

NEW FINDINGS

Purified intestinal epithelium from children newly diagnosed with IBD display distinct epigenetic and transcriptional alternations, which are partly retained in organoid cultures and correlate with disease outcome.

LIMITATIONS

Relatively small patient numbers require validation in additional cohorts.

IMPACT

Stable epigenetic alterations in the intestinal epithelium of children with IBD may explain variations in disease outcome and have potential to be developed into disease prognostic biomarkers in the future.

pediatric patients with IBD compared with controls. These data indicate that IECs undergo changes during IBD development and could be involved in pathogenesis. Further analyses of primary IECs from patients with IBD could improve our understanding of the large variations in disease progression and outcomes.

Keywords: Epigenetics; Intestinal Epithelium; Gut Microbiota; Human Intestinal Organoids.

Inflammatory bowel diseases (IBD) cause chronic relapsing inflammation that can affect any segments of the digestive tract (ie, Crohn's disease [CD]) or be restricted to the colon (ulcerative colitis [UC]).^{1,2} Although these diseases can manifest at any age, approximately one quarter of patients³ are diagnosed in childhood or early adulthood, when the disease course and subsequent outcomes can be particularly severe.³

The etiology of IBD is multifactorial, although the interplay of factors is still poorly understood. Large-scale genome-wide association studies have helped to characterize the genetic risk, identifying over 200 disease-associated loci.^{4,5} The striking overlap of genetic risk loci between CD, UC, and other immune-mediated diseases strongly suggests common immune regulatory pathways are affected in these conditions.^{4,5} However, current estimates of the overall genetic contribution to IBD risk are still only 13% for CD and 8% for UC. The rapid increase in the incidence of IBD in recent decades,⁶⁻⁸ the stability of the human genome, the dysbiosis of the gut microbiome,⁹⁻¹² as well as epidemiologic evidence, all suggest an association between the rise in IBD and the recent changes in our environment.

Epigenetic mechanisms operate at the interface between genetic predisposition and our environment, capable of causing stable, potentially heritable changes of cellular

function in response to environmental triggers.^{13,14} Consequently, epigenetics is being increasingly recognized as a highly plausible mechanism that may both initiate and then maintain intestinal mucosal inflammation in human IBD. A growing number of studies have reported IBD-associated alterations in epigenetic profiles, as well as associated changes in gene expression and/or cellular function. For example, DNA methylation (DNAm) changes in mucosal biopsies and peripheral blood mononuclear cells of both adults and children diagnosed with IBD have been demonstrated.^{15,16} However, the vast majority of studies were performed on mixed cell tissue samples (eg, whole blood, peripheral blood mononuclear cells, or mucosal biopsies)^{Q3} and, possibly because of changes in cellular composition, demonstrated a strong effect of inflammation on the observed epigenetic changes. Importantly, advances made by epigenetic consortia such as ROADMAP,¹⁷ BLUEPRINT,¹⁸ as well as single-cell RNA sequencing, have all demonstrated the importance of studying individual, disease-relevant cell types to best identify molecular alterations involved in pathophysiology.

Genetic and functional studies predominantly using mouse models and cell lines¹⁹⁻²¹ have provided strong evidence for impaired function of the intestinal epithelium in IBD. Yet, these models have done little to explain how the complex interplay between environmental factors, host genetics, intestinal cell function, and the adjacent microbiome lead to the development of the IBD phenotype and its subsequent evolution. To better elucidate specific alterations in this jigsaw, a genome-wide multi-layered omics approach of carefully selected primary cell samples is required. Importantly, in addition to unravelling novel aspects of disease pathogenesis, this approach in disease-relevant cell types (ie, the intestinal epithelium) could provide clinically relevant information. For example, in children and adults with IBD, it can be difficult to confidently distinguish CD from UC, with many patients remaining 'unclassified' despite disease progression. Intestinal epithelial cell (IEC)-specific 'omics' signatures have the potential to more rapidly and accurately diagnose the patient and, hence, improve the specificity of treatment management. Furthermore, variations of cell type-specific molecular profiles amongst IBD patients may be indicative of disease sub-phenotype and could therefore help to understand the large variations in disease behavior and outcome.

*Authors share co-first authorship ; § Authors share co-senior authorship.

Abbreviations used in this paper: AC, ascending colon; AUC, area under the concentration-time curve; CD, Crohn's disease; DMP, differentially methylated position; DEG, differentially expressed gene; DMR, differentially methylated region; DNAm, DNA methylation; FDR, false discovery rate; IBD, inflammatory bowel disease; IEC, intestinal epithelial cell; MDS, multidimensional scaling; rDMR, regulatory DMR; ROC, receiver operator characteristic; SC, sigmoid colon; TI, terminal ileum; UC, ulcerative colitis; WGCNA, Weighted Gene Co-expression Network Analysis. ^{Q2}

© 2018 by the AGA Institute. Published by Elsevier Inc. This is an open access article under the CC BY license (<http://creativecommons.org/licenses/by/4.0/>).

0016-5085

<https://doi.org/10.1053/j.gastro.2017.10.007>

Therefore, we simultaneously profiled genotype, epigenotype (ie, DNAm), gene expression, and the adjacent gut microbiome of highly purified IEC, obtained from children newly diagnosed with IBD and a matched cohort of non-IBD controls. We analyzed genome-wide 'omics' layers for potential IBD-specific alterations and functional consequences, as well as cross-talk between layers. Additionally, we generated intestinal epithelial organoids from patient biopsy samples and investigated their epigenetic profiles. Lastly, we applied statistical models to genome-wide datasets to test their ability to distinguish between disease subtypes, as well as potential correlation with disease outcome measures.

Methods

Patient Cohort

A cohort of 66 treatment-naïve children at diagnosis of their IBD, along with 30 age- and sex-matched non-inflammatory control children, were recruited by the Paediatric Gastroenterology team at Addenbrooke's Hospital during 2013–2016. This study was conducted with informed patient and/or carer consent as appropriate, and with full ethical approval (REC-12/EE/0482). Sample and patient details are provided in [Supplementary Tables 1 and 2](#). Children with macroscopically and histologically normal mucosa who had a diagnosis of IBD ruled out served as the non-disease control group. Each patient's final clinical diagnosis was based on the revised Porto criteria.²² At the diagnostic colonoscopy, additional mucosal biopsies were taken from the small bowel (ie, terminal ileum [TI]) and 2 large bowel sections (ie, ascending colon [AC] and sigmoid colon [SC]). A blood sample was taken for patient genotyping. Clinical phenotype and outcome data were prospectively recorded over a minimum of 18 months post-diagnosis ([Supplementary Table 1](#)). The inflammation status of a sample (inflamed vs non-inflamed) was based on the histology of a paired sample taken within 2 cm of samples at the time of the initial endoscopy. Longitudinal samples were taken from the TI and SC of a subset of patients that underwent repeat endoscopy (CD: n = 14; UC: n = 9).

Purification of Intestinal Epithelium

Biopsy samples were processed immediately and IECs purified using enzyme digestion and magnetic bead sorting for the epithelial cell adhesion molecule as described previously.^{16,23} Mucus for the isolation of adjacent microbiota was collected during tissue processing from sieve and centrifugation supernatant, then pooled, pelleted, and stored at -80°C to extract DNA from the adjacent microbiota. Further information is provided in the supplementary materials.

Human Intestinal Epithelial Organoid Culture

Intestinal organoids were generated from mucosal biopsies by isolation of intestinal crypts and culturing as described previously and detailed in the [Supplementary Methods](#) section and [Supplementary Table 4](#).²⁴

DNA and RNA Extraction

DNA and RNA were extracted simultaneously from the same sample using the AllPrep DNA/RNA mini kit (Qiagen).

DNA from the adjacent microbiota was extracted using QIAamp DNA Stool Mini Kit and from whole blood using the DNeasy Blood and Tissue Kit (both Qiagen). DNA was bisulfite-converted using Zymo DNA methylation Gold kit (Zymo Research).

Arrays and Sequencing

Genome-wide DNA methylation was profiled using the Illumina Infinium HumanMethylation450 and EPIC BeadChip platforms (Illumina, Cambridge, UK; Accession Numbers: E-MTAB-5463). Sample numbers are provided in [Supplementary Table S3](#). Expression profiling was performed using RNA-sequencing (RNA-seq) at the University of Kiel, Germany using an established pipeline as described previously.¹⁰ (Project accession number: E-MTAB-5464). Patient genotyping was performed using the Illumina OmniExpressExome-8 BeadChip Kit. 16S rRNA gene profiling of the adjacent microbiota was performed at the Wellcome Trust Sanger Centre (Hinxton, Cambridge). The 16S microbiota data can be found under EBI study ID PRJEB6663. For further details of the arrays and sequencing, please see the [Supplementary Methods](#).

Locus-specific validation of DNA methylation profiles was performed on bisulfite-converted DNA after polymerase chain reaction amplification using the Pyromark Q24 (Qiagen) pyrosequencing system as described previously.¹⁶

Bioinformatics Analyses

Extensive details of the bioinformatics methods used in this publication are described and referenced in the [Supplementary Methods](#). Briefly, DNAm analyses were performed using minfi,²⁵ sva,²⁶ DMRcate,²⁷ and limma²⁸ R packages. RNA-seq data was processed using established workflows.¹⁰ Microbiota composition analysis was performed using QIIME and phyloseq.²⁹ Differential analysis was performed using limma²⁸ for DNAm data (false discovery rate [FDR] <0.01) and DESeq2³⁰ for gene expression data (FDR <0.01 and log fold change >±0.5). InnateDB³¹ and the Reactome pathways were used to perform pathway enrichment analysis for the disease signatures identified from omics data layers. The diagnostic potential of omics data layers was tested using random forest classification models. Diagnostic accuracy was assessed via area under the concentration-time curve (AUC), precision scores, and receiver operator characteristic (ROC) curves. Weighted Gene Co-expression Network Analysis (WGCNA)³² was applied to gene expression and DNAm data for each diagnosis (CD and UC) by gut segment to correlate omics datasets with clinical phenotypic variables.

Results

DNA Methylation and Gene Expression Profiling of Purified Intestinal Epithelium Reveals Gut Segment-specific and Disease-associated Alterations

To investigate IEC pathophysiology in pediatric IBD, we first performed unsupervised analysis of genome-wide DNAm, gene expression, and 16S microbial profiles generated from a total of 170 samples ([Figure 1A](#) and [Table 1](#)). Multidimensional scaling (MDS) plots indicate sample

Q7

Q8

Q9

Q10

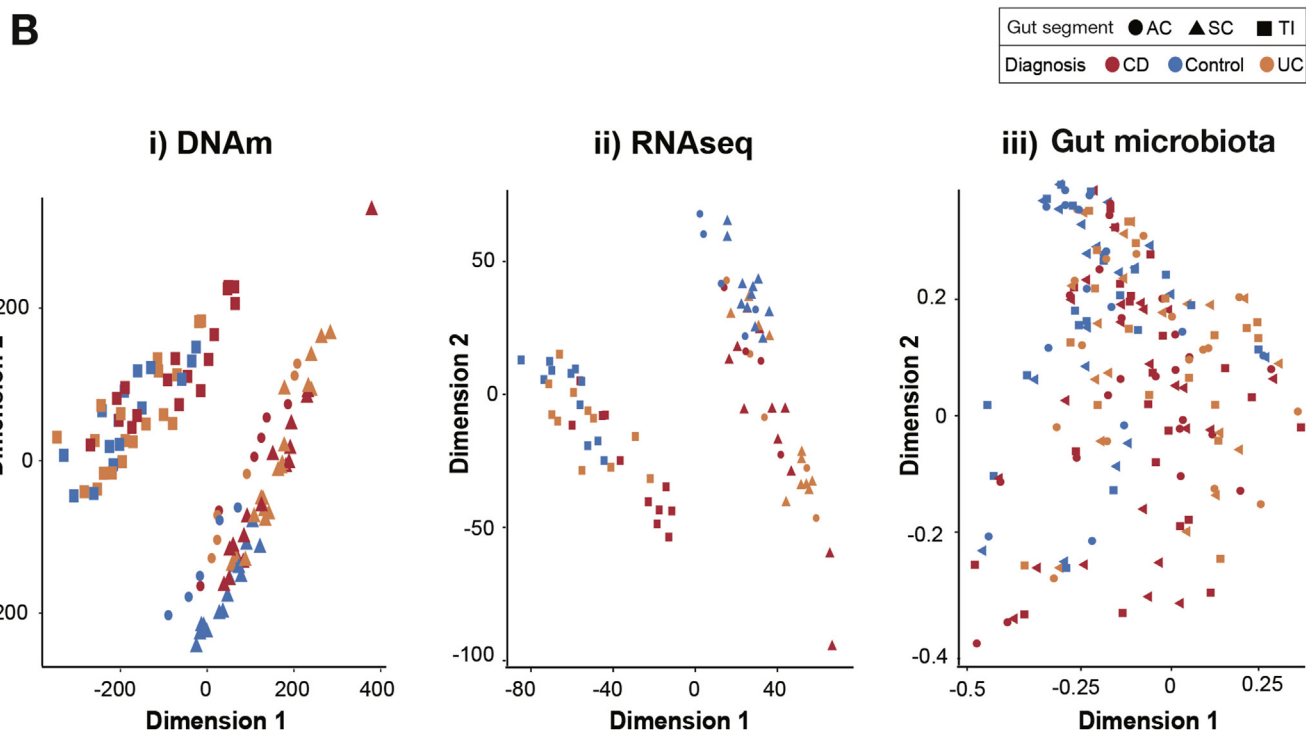
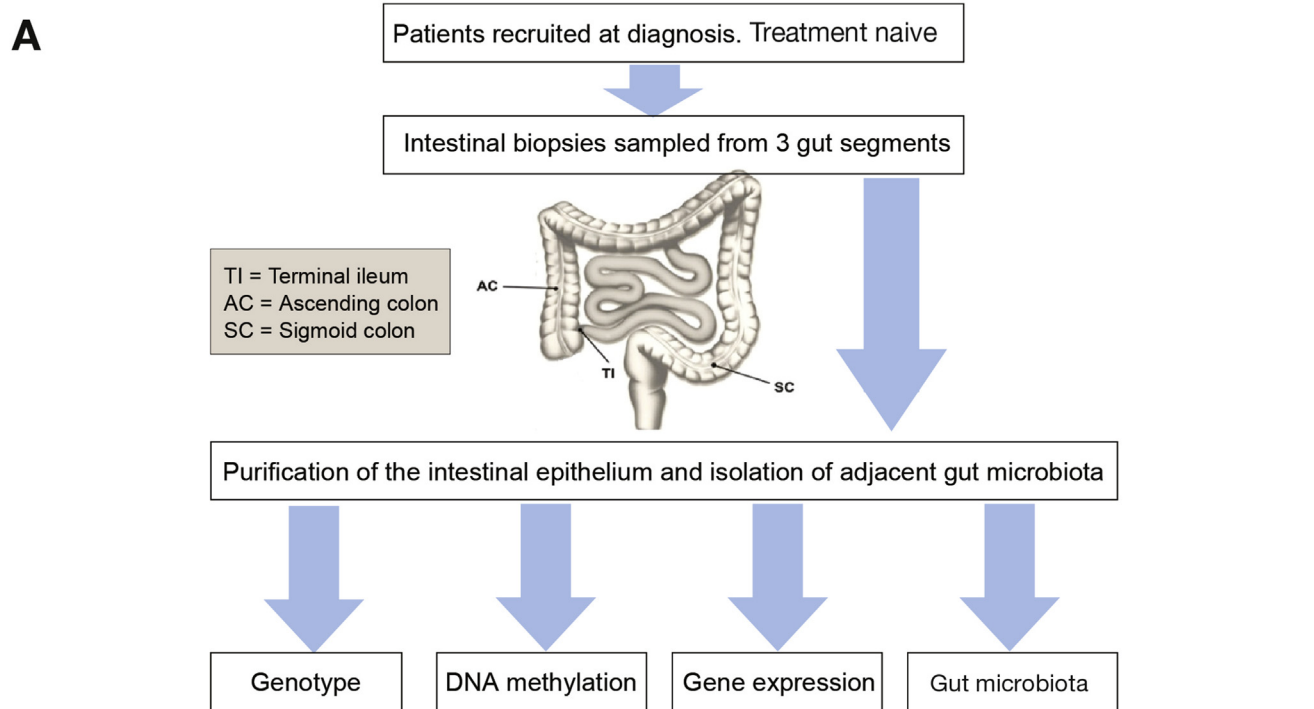


Figure 1. Overview of study design and multi-dimensional scaling (MDS) analysis of genome-wide datasets. (A) Outline of study design. (B) MDS plots for each dataset: (i) DNAm based on batch corrected M-values; (ii) r-log normalized RNAseq gene expression counts; (iii) gut microbiota 16S operational taxonomic units normalized counts. Samples are labelled according to diagnosis (CD, Crohn's disease; UC, ulcerative colitis; control) and gut segment. Schematic in part A adapted from Tauschmann et al.⁴¹

similarity/differences based on all data points included. MDS plots of DNAm and gene expression profiles revealed distinct clustering of samples by gut segment separating all

TI-derived epithelium from colonic (ie, AC and SC) samples (Figure 1Bi and 1Bii). Moreover, samples derived from controls clustered closely both on an epigenetic (DNAm)

Table 1. Summary of Patients, Samples, and Generated Datasets

	DNAm			RNAseq			16S sequencing			Genotype
	TI	AC	SC	TI	AC	SC	TI	AC	SC	
Total samples at diagnosis	162			81			170			62
Total individuals	73	15	74	33	15	33	58	53	59	62
CD	31	5	32	11	5	11	21	21	22	24
450K cohort	13	5	13							
EPIC cohort	17		18							
Organoids	5		5							
UC	18	5	18	11	5	11	18	16	18	18
450K cohort	13	5	13							
EPIC cohort	5		5							
Controls	24	5	24	11	5	11	19	16	19	20
450K cohort	14	5	14							
EPIC cohort	3		3							
Organoids	7		7							
Repeat endoscopies										
UC	9		9							
CD	14		14							

AC, ascending colon; CD, Crohn's disease; SC, sigmoid colon; TI, terminal ileum; UC ulcerative colitis.

and transcriptomic level for each gut segment. Interestingly, IBD-derived samples displayed more variation, with a subset of IBD samples distinctly separating from controls (Figure 1Bi, Bii and Supplementary Figure 1). In contrast to DNAm and gene transcription, no clear separation was evident from the 16S microbial community profiles using the same MDS approach (Figure 1Biii). However, analysis of the bacterial operational taxonomic unit by family abundance and alpha-diversity did reveal variation by gut segment (Supplementary Figure 2) and reduction in species diversity for CD patients (Supplementary Figure 2).

Taken together, initial unsupervised analysis of genome-wide intestinal epithelial profiles reveals highly gut segment-specific signatures and suggests disease-associated alterations of DNAm and gene expression.

Disease-specific Alterations in IEC Epigenetic and Transcriptional Profiles are Partly Independent of Inflammation Status

Given the distinct clustering patterns we observed on a genome-wide scale, we next used a variance component model to assess the relative contribution of diagnosis and inflammation to the observed variance within each data layer, by gut segment. As shown in Figure 2A, the variation explained by disease (ie, diagnosis) exceeds that of inflammation in the majority of datasets. This highlights the presence of disease-specific molecular alterations, which are partly independent of the current inflammatory activity. Full results of the variance decomposition analysis can be found in Supplementary Figure 3. To extend these findings, we performed separate differential analysis (gene expression and DNAm) of inflammation and disease in the colonic epithelium. This allowed us to identify, for each CpG site or gene, the relative significance of inflammation and disease. Results showed that a majority of the differentially

methylated positions (DMPs) between CD or UC and controls are primarily driven by diagnostic status and not inflammation (FDR <0.01, Figure 2B and C). Similarly, diagnosis explained 74% and 82% of the differentially expressed genes (DEGs) for CD and UC, respectively (Figure 2D and E).

Additionally, generating MDS plots by labelling samples according to gut segment, diagnosis, and inflammatory status did not show a clear separation between inflamed and non-inflamed samples (Supplementary Figure S1). Lastly, we also tested for the potential impact of inflammation on cellular composition in our purified samples by generating a gene expression heat map of common epithelial and immune cell marker genes (Supplementary Figure S4). Although a number of genes were found to be differentially expressed between IBD and control samples (eg, DEFA5, DEFA6, LYZ, PLA2G2A, CD40, CD44), none of the marker genes correlated with inflammatory status, suggesting minimal impact of epithelial cell composition and immune cell contamination on the observed disease-specific molecular changes (Supplementary Figure S4).

In summary, these analyses demonstrate the presence of clear epigenetic, transcriptomic, and adjacent microbial alterations in the intestinal epithelium of children newly diagnosed with IBD, with a proportion being independent of intestinal inflammation.

Differential Methylation Analysis Reveals Disease-specific Signatures That Affect Gene Transcription

Next we performed differential DNAm and gene expression analyses by comparing control, CD-, and UC-derived datasets for each gut segment. When performing these analyses, inflammation was controlled for within the differential analysis thereby allowing us to focus on

541
542
543
544
545
546
547
548
549
550
551
552
553
554
555
556
557
558
559
560
561
562
563
564
565
566
576
577
578
579
580
581
582
583
584
585
586
587
588
589
590
591
592
593
594
595
596
597
598
599
600

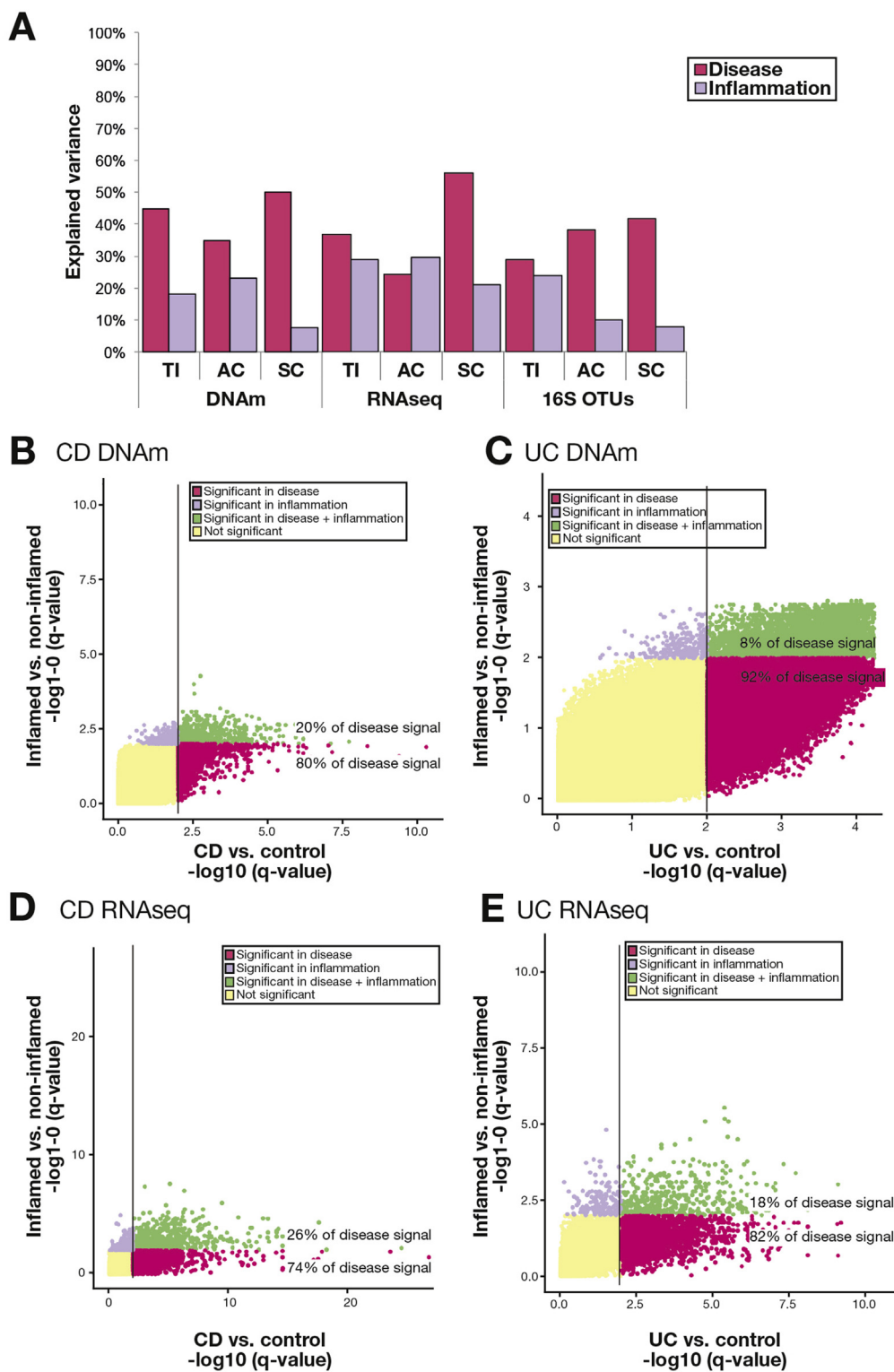


Figure 2. Contribution of diagnosis and inflammation to variance within each data layer. (A) Bar chart of the explained variance by diagnosis and inflammation across each dataset separated by gut segment. (B–E) Scatterplot of P values derived from differential DNAm (I and I) and gene expression (I and I) in sigmoid colon (SC) samples. For each CpG or gene, P values were generated for the comparison between Crohn's disease (CD)/ulcerative colitis (UC) and control, and inflammation status (ie, inflamed vs non-inflamed). CpGs and genes with significant P values are plotted in purple for inflammation, in red for diagnosis, and in green if significant for both comparisons. Adjusted $P < .01$ was considered as significant.

molecular alterations that occur in relative independence of mucosal inflammation. Additionally, in an attempt to connect epigenetic and transcriptomic signatures, we identified differentially methylated regions (DMRs) that were located within 10kb of the transcription start site of a DEG. Such regions were termed regulatory DMRs (rDMRs).

Analysis of ileal IECs revealed CD-specific changes in both DNAm (Figure 3Ai and Supplementary Tables 5 and 6) and gene expression (Figure 3Aii and Supplementary Tables 7 and 8), when compared with either controls or UC, with a proportion overlapping between the 2 comparisons. In contrast, no significant DMPs or DEGs were

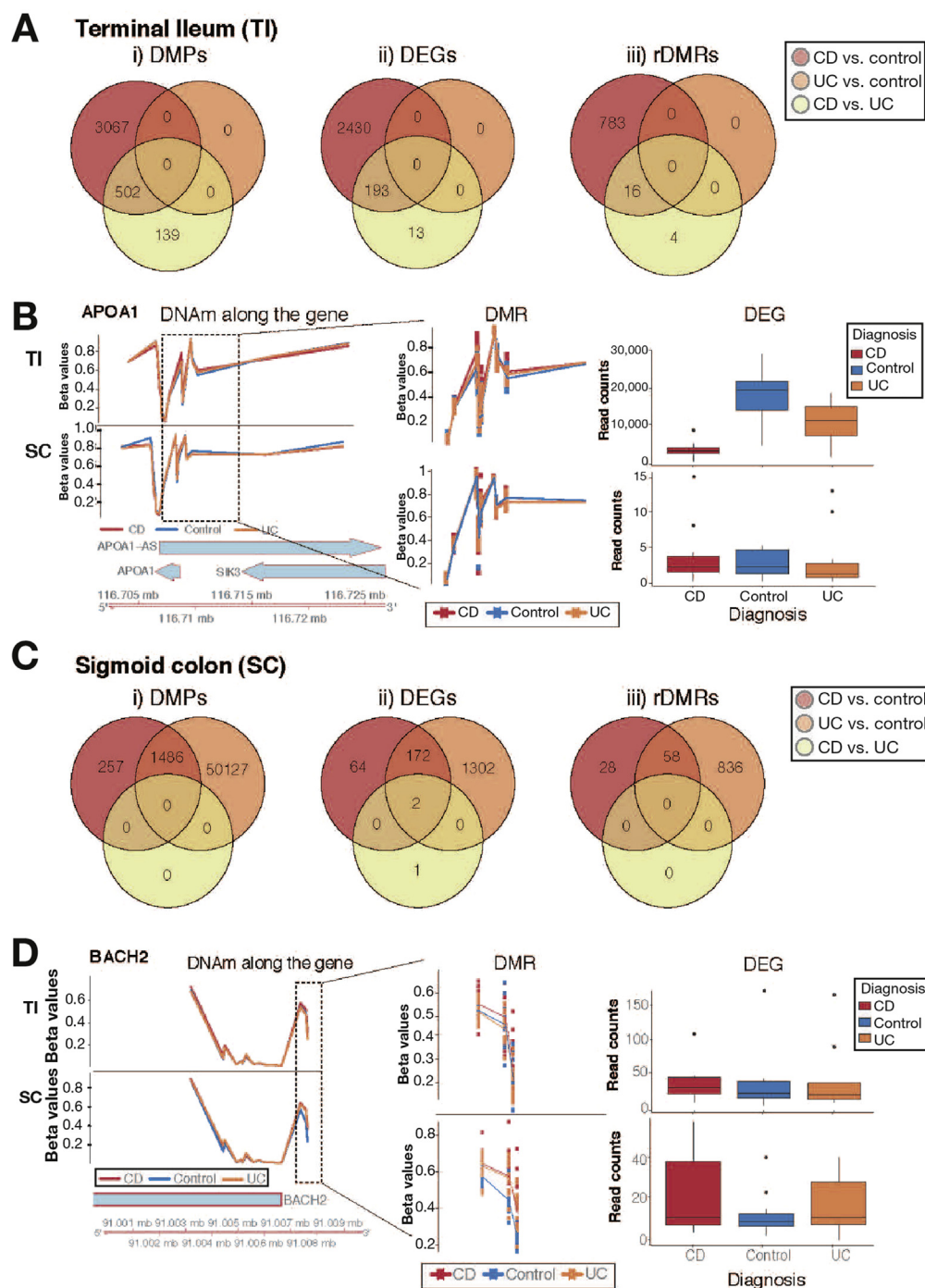


Figure 3. Differential DNAm and gene expression analysis were performed separately for terminal ileum (TI) (A and B) and sigmoid colon (SC) (C and D), taking mucosal inflammation into account. (A and C) Venn diagrams of significant differentially methylated positions (DMPs), differentially expressed genes (DEGs), and regulatory DMRs (rDMRs). (B and D) Example of disease-specific rDMRs displaying DNA methylation levels expressed as Beta value on the y-axis in the left panel separately for TI and SC samples in the upper and lower panel, respectively. Beta value of 0 represents un-methylated, while 1 represents fully methylated CpG site. Genomic location is indicated on the x-axis. The middle panel displays identified rDMR (enlarged). The right panel displays a boxplot of the respective gene expression according to diagnosis. (B) rDMR within the APOA1 identified in TI-derived epithelium of children diagnosed with CD. (D) rDMR within the BACH2 gene identified in colonic IEC.

identified when comparing UC with controls. Importantly, amongst identified rDMRs, several have previously been reported to be associated with IBD (eg, CASP1³³ and APOA1⁹) (Figure 3B).

Contrary to the ileum, changes observed in the SC reflected a 'common IBD' signature, with a major overlap between UC and CD signatures and only a single significant DEG (RARRES3 [Retinoic Acid Receptor Responder 3]) identified between the 2 diagnoses (Figure 3C and Supplementary Tables 9-14). RARRES3 is thought to have

growth inhibitory and cell differentiation activities. One example of an rDMR that jointly affects CD and UC in the colon is BACH2 (Figure 3D), a transcription regulator, where a decrease in DNAm matched the increase in gene expression levels in both CD and UC patients. Interestingly, a proportion of the CD-related changes identified in TI samples were also found to be present in SC samples (Supplementary Figure 5).

Overall, these results indicate that CD-specific DNAm and gene-expression changes are present in ileal IECs. In

781
782
783
784
785
786
787
788
789
790
791
792
793
794
795
796
797
798
799
800
801
802
803
804
805
806

BASIC AND
TRANSLATIONAL AT

print & web 4C/FPO
q18

816
817
818
819
820
821
822
823
824
825
826
827
828
829
830
831
832
833
834
835
836
837
838
839
840

contrast, molecular changes observed in the colonic epithelium revealed a major overlap between CD and UC, reflecting a 'common IBD' signature.

Pathway Enrichment Analysis of Identified rDMRs Reveal Both Common IBD and Disease-specific Pathways

The intestinal epithelium serves a wide range of functions as a physical, chemical and immunological barrier and a bridge between the innate and adaptive immune response.³⁴ We used pathway enrichment analysis to investigate functional pathways (of rDMRs) that may be altered at diagnosis in a child with IBD. A wide variety of immune system-, metabolism-, and signal transduction-related pathways were significantly enriched (Figure 4). Many of the immune system-related pathways (eg, interferon signaling and immuno-regulatory interactions) are shared between the gut segments and diagnoses; suggesting common alterations are present in IBD. Moreover, several of the significantly enriched pathways have previously been implicated in either IBD pathogenesis or IEC function (Figure 4).

IBD-associated intestinal Epithelial-specific Epigenetic Alterations are Stable Over Time and Partly Retained in Ex-vivo Organoid Culture

Next, we investigated the stability of IEC DNAm profiles in IBD patients over time. We obtained ileal and colonic biopsies (SC) from IBD patients both at diagnosis and at a later stage in their disease (n = 14 CD, n = 9 UC). Strikingly, CD- and UC-associated DMPs showed remarkable stability over time, demonstrated by the strong correlations of the methylation values at diagnosis and repeat endoscopy within each gut segment (Figure 5A and Supplementary Figure 6). This was in spite of changes to the underlying mucosal inflammatory status (see Supplementary Table 1). To further test the stability and potential inflammation independence of disease-specific epigenetic alterations in IBD-derived IEC, we generated patient-derived intestinal organoids from an additional cohort of children newly diagnosed with CD (n=5) and matched healthy controls (n=7). Expansion of mucosal crypts from TI and SC in culture gave rise to 3-dimensional organoids (Figure 5B). Organoids derived from CD patients did not differ in their

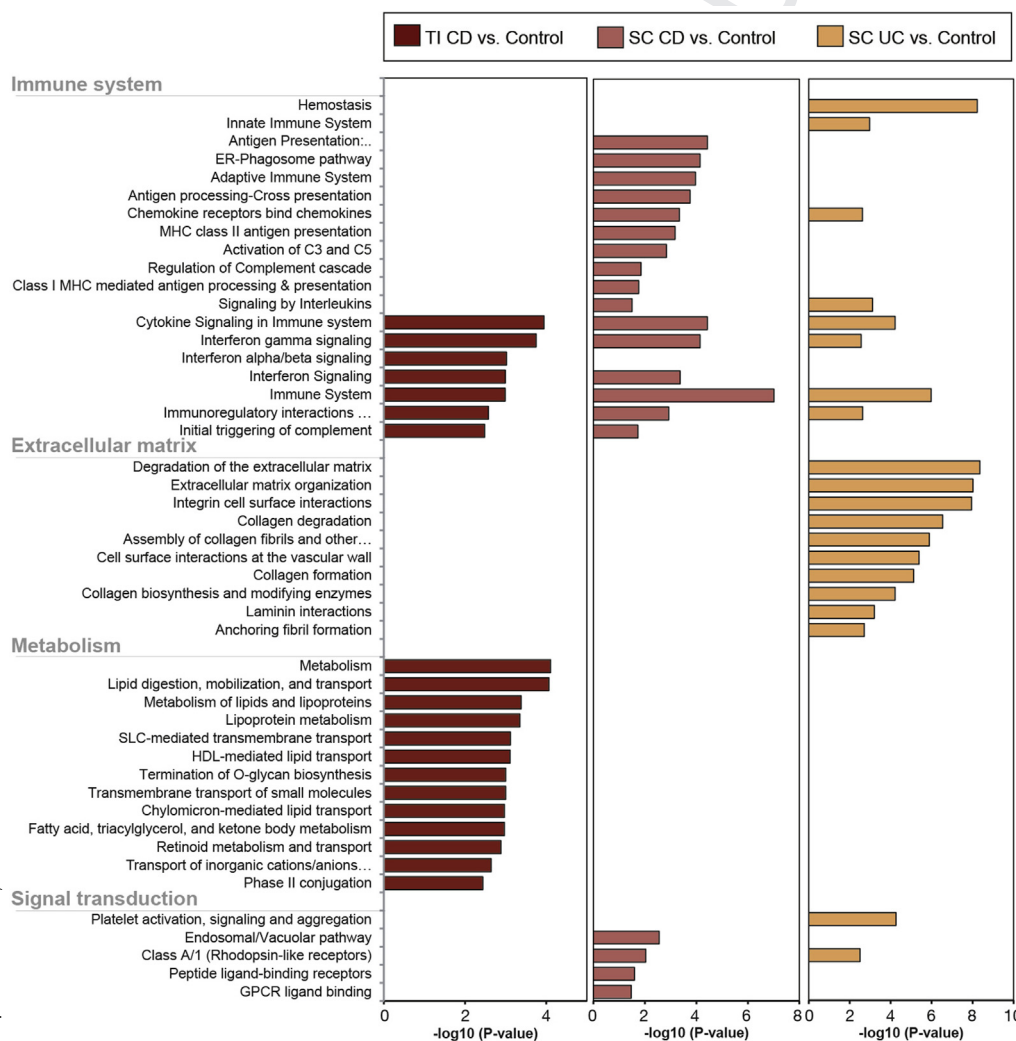


Figure 4. Pathway enrichment analysis of disease-specific regulatory DMRs (rDMRs). Pathway enrichment analysis was performed on identified rDMRs derived from the 3 comparisons between Crohn's disease (CD) vs controls in terminal ileum (TI) and sigmoid colon (SC) samples (left and middle panel) and ulcerative colitis (UC) vs controls in SC samples (right panel). Analysis was performed using InnateDB and Reactome database and significant enrichment of individual pathways is displayed as the $-\log_{10}$ (adjusted P value).

microscopic appearance or culturing behavior from those derived from healthy controls (Figure 5B). However, assessing their genome-wide DNA methylation profiles revealed distinct alterations, suggesting that they retain a proportion of disease-associated epigenetic changes. Despite the relatively small sample number, CD-associated DMPs (ie, identified in Figure 3) showed a clear trend to be also differentially methylated in CD-derived compared with control organoids. This was indicated by the presence of inflated *P* values (larger difference between observed vs expected *P* values) of CD-associated DMPs compared with randomly selected CpGs (Figure 5C). Using locus-specific pyrosequencing, we were able to validate a subset of CD-specific DMPs that were retained in organoid cultures (Figure 5D and 5E).

Together, these data demonstrate that disease-associated epigenetic alterations in the intestinal epithelium are stable over time and are at least in part retained in ex-vivo organoid cultures.

Intestinal Epithelial DMRs, DEGs, and rDMRs are Enriched Around Genetic IBD Risk Loci

Genome-wide association studies have successfully identified over 200 loci predisposing to IBD.^{4,5} However, limited information is currently available on the potential mechanisms involved in mediating genetic risk and/or which cell types are particularly affected. Here we used our epithelial cell-derived molecular signatures to test for an enrichment of disease-specific DMRs, DEGs, and rDMRs within genomic IBD risk loci. We observed highly significant enrichment of DMRs, DEGs, and rDMRs in both colonic and ileal IECs for IBD risk loci, while limited enrichment was found for genetic variants that have been linked to other multifactorial diseases with an immune-mediated pathogenesis, such as Type 1 diabetes and multiple sclerosis (Supplementary Figure 7). Together these results suggest that interactions between the IBD risk loci and DNAm and/or transcription may occur in children carrying disease variants.

IEC DNA Methylation and Gene Expression Signatures Accurately Predict Disease Status and Correlate With Clinical Outcome Measures

Given the striking IBD-associated changes observed in intestinal epithelial DNAm and gene expression, we went on to test the ability of these signatures to predict diagnosis. Additionally, we hypothesized that variation observed within IBD-derived patient samples could be indicative of future disease behavior and outcome. To address these hypotheses, we applied a machine-learning model (random forest) to the individual omics data layers. The model identified those data points (eg, CpGs, genes, operational taxonomic units) that could predict disease status for each patient with high precision and accuracy (see Supplementary Methods section for further details). As demonstrated in Figure 6, DNAm data derived from either gut segment produced a model with a high AUC (>0.8) (Figure 6A). The best model separating disease from control

was based on DNAm data from the SC (AUC=0.94, CV=40)^{Q11} with sensitivity of 75% and specificity of 100% (Figure 6Ai and 6Aii). Importantly, the use of ileal DNAm datasets allowed separation between CD and UC with high precision (77%), sensitivity (57%), and specificity (93%) (AUC=0.92, CV=24) (Figure 6B). The accuracy of the TI DNAm signatures in distinguishing CD and UC was confirmed in a follow-up patient cohort, analyzed using a second DNAm array platform (Illumina EPIC array, see Methods and Supplementary Figure 8). Full details of the models, including AUC, sensitivity, and specificity, can be found in Supplementary Table 15. In contrast, models built using the IBD risk loci from our patient genotyping data yielded the lowest model score (AUC=0.49) (Figure 6Ai).

To correlate genome-wide IEC profiles with clinical outcome measures (including binary, numerical, and categorical parameters) we used a WGCNA approach. WGCNA identifies patterns within a given dataset (ie, RNAseq data) and combines genes or CpGs that vary similarly across samples into modules. Each of these modules was then tested for a significant correlation with clinical outcomes. The application of WGCNA to RNAseq data derived from the TI of CD patients led to the identification of several gene modules (ie, groups of genes) that correlate significantly (correlation $\geq \pm 0.6$, $P < .05$) with a number of disease outcome measures including the requirement for treatment with biologics and number of treatment escalations within the first 18 months following diagnosis (Figure 6C). Interestingly, modules correlating with disease outcome measures did not show any correlation with gender, age, or disease phenotype at diagnosis (eg, abdominal pain, diarrhea, and Pediatric Crohn's Disease Activity Index). Clustering all samples according to expression levels of genes within the strongest modules separated CD patients in 2 groups (Figure 6Di). Kaplan Meier curves for these groups demonstrated striking differences in both the requirement for biologics and time-to-third-treatment escalation (Figure 6Dii and 6Diii). In addition, we applied WGCNA to the DNAm data. Although the overall correlation of identified modules was less striking, separating samples according to DNAm profiles of the strongest module still demonstrated a significant difference in outcome measures between resulting patient groups (Figure 6Ei-6Eiii). Similar results were obtained from UC patient-derived signatures in SC samples (Supplementary Figure 9). Finally, comparing annotated genes from the top modules identified in RNAseq and DNAm datasets revealed an overlap of 57% and 79%, respectively, suggesting that expression signatures might be in part underpinned by stable epigenetic changes (Figure 6F). Based on these preliminary results, both DNAm and RNAseq data contain signatures that accurately predict disease status and correlate with selected disease outcome parameters.

Discussion

Substantial evidence suggests that impaired function of the intestinal epithelium plays a major role in IBD pathogenesis. However, our current understanding of the exact

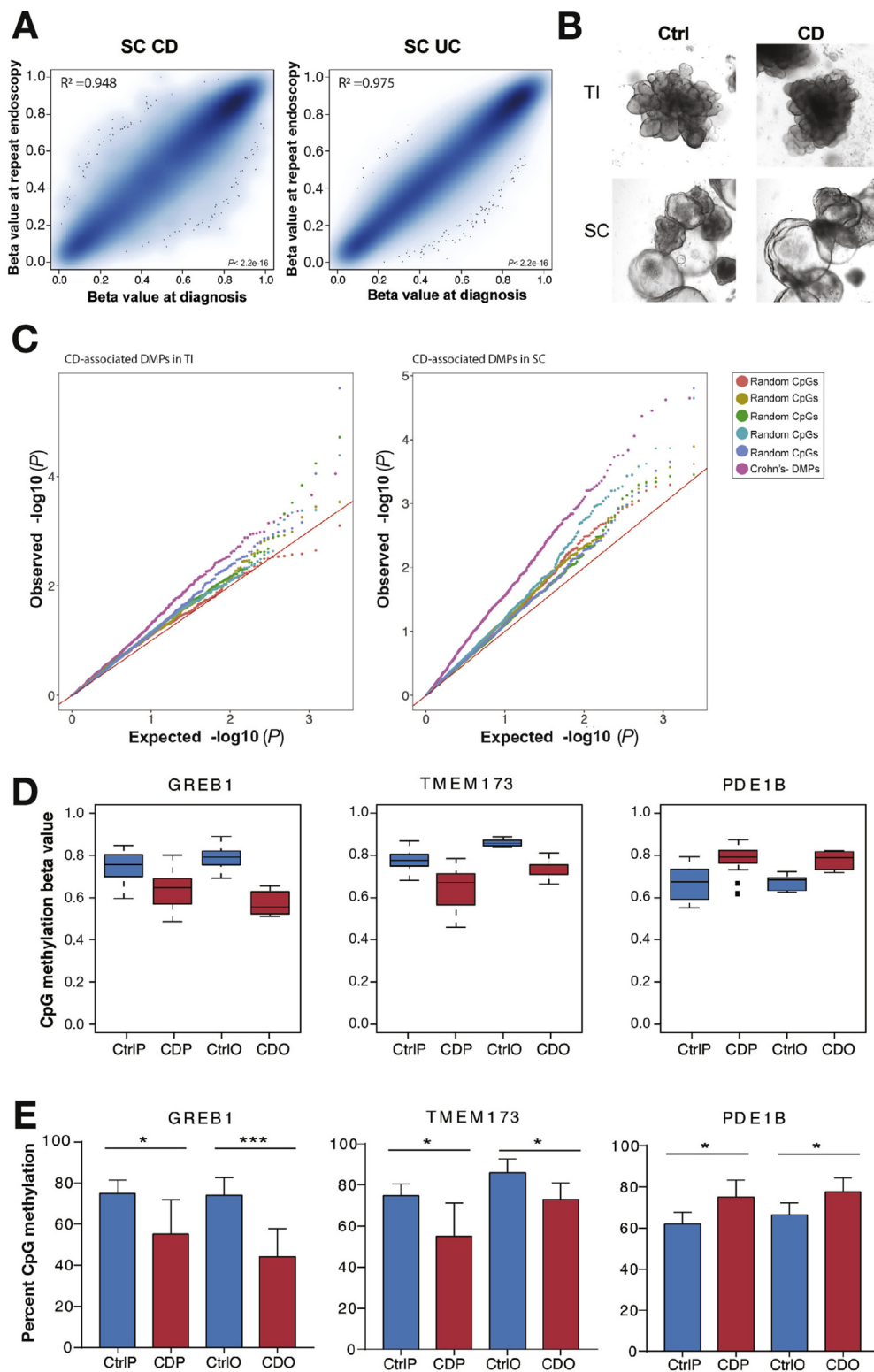
1021
1022
1023
1024
1025
1026
1027
1028
1029
1030
1031
1032
1033
1034
1035
1036
1037
1038
1039
1040
1041
1042
1043
1044
1045
1046

BASIC AND
TRANSLATIONAL AT

1056
1057
1058
1059
1060
1061
1062
1063
1064
1065
1066
1067
1068
1069
1070
1071
1072
1073
1074
1075
1076
1077
1078
1079
1080

mechanisms remains limited. It is also becoming increasingly clear that functional alterations in complex disease are likely to be caused by and/or result in a multifaceted interplay between several layers of cellular regulation.

Specific to the GI tract, the intestinal microbiota adds further complexity because it has been shown to influence cellular function of the intestinal epithelium both in health and IBD.^{9,10,12} Given the wide range of phenotypes and diverse



BASIC AND
TRANSLATIONAL AT

print & web 4C/FPO

spectrum of disease behavior within the conditions we currently label as CD and UC, we urgently require novel molecular signatures to allow better classification of clinically relevant disease entities.

Here, we applied a multi-omics profiling approach to a highly purified IEC sample set obtained from a prospectively recruited, treatment-naïve, pediatric patient cohort. Unsupervised analysis revealed fundamental differences in the methylation and gene expression profiles by gut segment.^{9,10,16} Moreover, within each gut segment, we observed distinct disease-specific variation in both DNAm and gene expression, which were found to be partly independent of the presence or absence of microscopic mucosal inflammation. Specifically, we found that the majority of DNAm and RNAseq disease signatures from the SC were not primarily explained by inflammation status. This strongly suggests that there are underlying epigenetic and transcriptomic changes within IECs in IBD patients, which are present irrespective of inflammatory activity. Our findings further expand on previous studies using whole gut biopsies, which reported major transcriptional or epigenetic changes that were primarily associated with the presence of mucosal inflammation.^{9,10} Although we also observed a strong, inflammation-associated signal, purification of the intestinal epithelium (and thereby removal of infiltrating immune cells) has allowed identification of a cell type-specific signature that does not seem to be exclusively driven by mucosal inflammation.

In contrast to genome-wide DNAm and gene transcription profiles, unsupervised MDS analysis of our 16S data did not show any specific sample clusters and/or clear association with key phenotypes such as gut segment, disease entity, or inflammation. This is most likely because of the large inter-individual and intra-individual variation; an observation that has been previously reported by others.^{9,11,12} However, supervised analyses revealed gut segment as well as disease-associated changes in microbial composition. Analysis of the 16S data in combination with the epithelial omics data was unable to identify strong correlations between DEGs and 16S abundances or dose-dependent relationships for subgroups of patients. Nevertheless, we consider the fact that our 16S data was generated from microbes isolated from individual gut segments as novel and therefore potentially highly valuable as reference for future work in this rapidly evolving field.

Further investigating disease-specific DNAm and gene expression changes, we were able to identify a number of

significant DEGs and DMRs, a proportion of which overlapped (rDMRs), indicating a functional interconnection between the 2 data layers. Reassuringly, a number of identified genes had previously been reported, including APOA1¹² and CASP1.⁹ When comparing identified DMRs, DEGs, and rDMRs, we discovered that significant changes in the TI were only present in CD-derived samples. In contrast, analysis in the colonic epithelium showed both CD- and UC-specific changes, which also displayed a major overlap likely reflecting common phenotypic features shared between the 2 conditions. Together these data suggest the presence of a CD-specific signature in the TI epithelium and a common IBD signature in the SC. The identification of shared, enriched pathways for the 2 diagnoses further supports this hypothesis. Additionally, enrichment for pathways implicated in the cross-talk between cells of the innate and adaptive immune response highlights the important role of the intestinal epithelium in orchestrating intestinal host defense and suggests that alterations in these key processes may lead to the initiation and/or persistence of gut inflammation in IBD.

The impact of the observed IEC-specific epigenetic alterations on IBD pathogenesis will depend at least in part on the stability of such molecular signatures. Investigating IEC DNAm profiles of the same patient at 2 time points (ie, at diagnosis and at later disease stage) allowed us to demonstrate the strikingly high stability of disease-associated methylation signatures in small bowel and colonic IEC. This was despite changes in medication and mucosal inflammation over a period of up to 20 months. These findings suggest that stable epigenetic alterations may contribute to chronic relapsing inflammation by mediating altered IEC function. Interestingly, CD-derived epithelium appeared to retain a degree of disease-specific alterations even when cultured ex-vivo as organoids, further highlighting both their stability and relative independence of mucosal inflammation. Additionally, our findings add further support to recent reports on patient-derived intestinal organoids to be used as novel translational research tools.³⁵

Despite the major success of genome-wide association studies in identifying disease-predisposing genetic loci, information on the functional consequences and cell specificity remain limited. Expression quantitative trait loci have been identified for a subset of the IBD risk loci from whole biopsies³⁶ and blood cell subsets.³⁷ More recently,

Figure 5. Stability of disease-associated intestinal epithelial DNA methylation changes: (A) Correlation plot of DNA methylation (Beta values) of disease-associated differentially methylated positions (DMPs) at diagnosis and at repeat endoscopy for each patient at the 2 time points. Shown are Crohn's disease (CD)-associated DMPs (left) and ulcerative colitis (UC)-associated DMPs (right) in sigmoid colon (SC) epithelium (adjusted $P < .01$). (B) Brightfield microscopic images of fully grown intestinal epithelial organoids derived from 2 gut segments (ie, terminal ileum [TI] and SC) of CD and control patients. (C) Quantile-quantile plot generated from organoid-derived genome-wide DNAm P values. Plotted are P values (observed vs expected) comparing specific CD-associated DMPs (from Figure 3) for each gut segment with randomly selected CpGs. (D) Examples of CD-associated DMPs being retained in patient-derived organoids. Plotted are beta values derived from genome-wide array data generated from purified colonic epithelium and respective organoids. GREB1, Growth Regulation By Estrogen In Breast Cancer 1; TMEM173, Transmembrane Protein 173; PDE1B, Phosphodiesterase 1B; CtrlP, Control purified IEC ($n = 14$); CDP, CD purified IEC ($n = 13$); CtrlO, Control organoids ($n = 7$); CDO, CD organoids ($n = 5$). (E) Validation of CpGs shown in D. Validation of genome-wide DNAm data using pyrosequencing. $n = 5-7$ per group; * $P < .05$; *** $P < .001$; unpaired, 2-tailed t -test between Ctrl and CD.

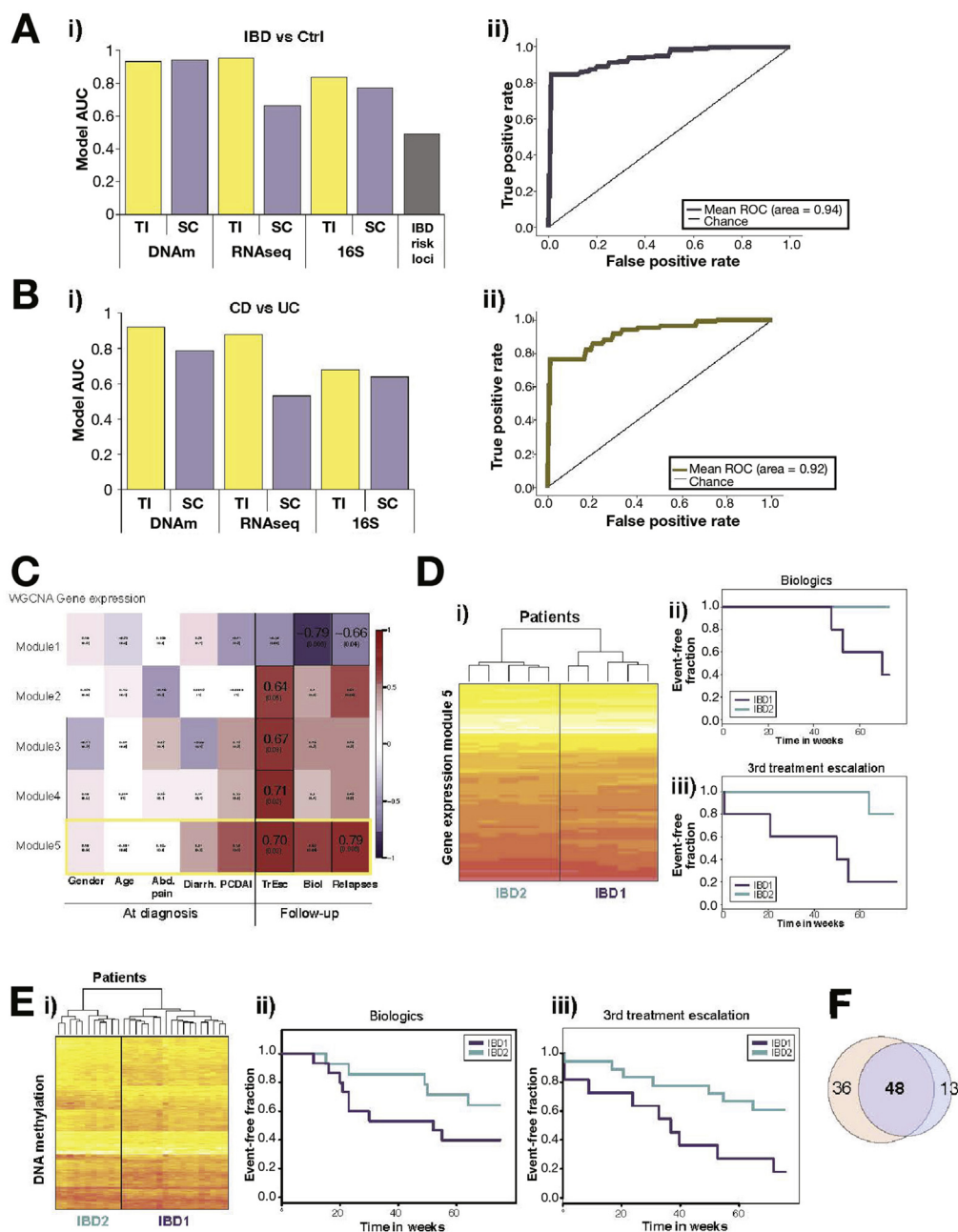


Figure 6. Correlation of intestinal epithelial cells (IEC)-specific molecular signatures with diagnosis and clinical outcome measures: IEC-derived epigenetic, transcriptomic, and microbial signatures were tested for their potential to predict diagnostic status (A and B) and correlation with disease outcome parameters (C–F). (A) Bar chart indicating area under the curve (AUC) of the best model to accurately differentiate samples based on diagnosis (ie, IBD vs controls). (Aii) ROC curve for the best diagnostic model (inflammatory bowel disease [IBD] vs control) using colonic DNAm data. (B) Bar chart of the AUC of the best models to differentiate between Crohn’s disease (CD) and ulcerative colitis (UC). (Bii) Receiver operator characteristic (ROC) curve for the best model separating CD from UC using ileal IEC DNAm data. (C) Weighted Gene Co-Expression Network Analysis (WGCNA) of CD terminal ileum (TI)-derived RNA-Seq data showing correlations between key gene-expression modules and clinical parameters. Each cell on the heatmap displays Pearson correlation coefficient and corresponding *P* value. Outlined cells indicate significant correlations. (D) Heatmap and hierarchical clustering of patients based on gene expression (ie, RNAseq counts) for strongest module. (Dii and Diii) Kaplan-Meier curves based on patient grouping derived from 7Di, ie, top gene expression module for use of biologics and time to third treatment escalation during 75 weeks of follow-up (*n* = 10 patients, *P* = .049 and *P* = .032, log-rank test). (E) Heat-map and hierarchical clustering of CpGs within strongest module identified by applying WGCNA to CD TI DNA methylation profiles. (Eii and Eiii) Kaplan Meier curves based on patient grouping derived from 7Ei for use of biologics (Eii) and time to third treatment escalation (Eiii) during 75 weeks follow-up (*n* = 29 patients, *P* = .025 and *P* = .043, log-rank test). (F) Venn-diagram showing the overlap between annotated genes that were present in the top modules for both gene expression and DNA methylation.

differences in DNAm and chromatin conformation³⁸ were also identified for a subset of the IBD risk loci in immune cells.³⁹ Our study adds further detail and specificity by demonstrating enrichment of disease-specific DMRs, DEGs, and rDMRS within IBD susceptibility loci^{4,5} in both gut segments.

An additional major strength of our prospectively recruited pediatric patient cohort was the availability of detailed phenotype and disease outcome data, allowing us to test for potential correlation between molecular signatures and clinical phenotypes. Despite the relatively small sample numbers included in these analyses, both the potential diagnostic and prognostic value of our IEC signatures is evident. While current diagnostic approaches are sufficient for most patients, a minority of patients require repeated and prolonged investigations to confirm a diagnosis. Additionally, it is frequently challenging to differentiate UC from CD in children, both at diagnosis and later in the disease course. Therefore, a diagnostic model to reliably differentiate CD from UC, such as the model built using DNAm data from the ileum with high sensitivity and specificity, could be of clinical value. Correlating genome-wide molecular signatures with clinical outcome measures continue to be a major challenge and a wide range of bioinformatics tools have been developed. We decided to utilize WGCNA, which has been successfully applied to both RNA-seq and DNAm datasets, allowing identification and correlation of individual gene modules with clinical parameters.⁴⁰ Results are highly encouraging because we discovered a number of gene expression modules that correlated strongly with the number of relapses and the requirement for treatment with biologics. Interestingly, overlapping modules derived from applying WGCNA to RNAseq data with those derived from DNAm data revealed a major overlap, suggesting prognostic expression signatures maybe at least in part underpinned by epigenetic changes.

As a limitation to our study, we acknowledge that the total number of patients included is relatively low and hence some of the analyses performed, particularly those that correlate signatures with clinical outcome, should be considered as preliminary. However, to the best of our knowledge this is the first and largest study applying a multi-omics profiling approach to a unique sample collection of highly purified intestinal epithelium. The fact that all patients were recruited at diagnosis (treatment-naïve) also represents an important strength. Last but not least, although our study was performed on a pediatric patient cohort, we consider our findings to be equally relevant to adult-onset IBD given the similarities in disease phenotype (particularly in teenage onset) and common concepts of disease pathogenesis.

In summary, our study is the first to apply a multi-omics profiling approach to a large collection of purified intestinal epithelial samples. The findings clearly demonstrate disease-specific abnormalities in epithelial cell function in children with IBD. We also highlight how specific data signatures might be indicative of disease status and behavior and therefore have a potential to be of clinical relevance in the future.

Supplementary Material

Note: To access the supplementary material accompanying this article, visit the online version of *Gastroenterology* at www.gastrojournal.org, and at <https://doi.org/10.1053/j.gastro.2017.10.007>.

References

1. Baumgart DC, Sandborn WJ. Inflammatory bowel disease: clinical aspects and established and evolving therapies. *Lancet* 2007;369:1641–1657.
2. Liu JZ, van Sommeren S, Huang H, et al. Association analyses identify 38 susceptibility loci for inflammatory bowel disease and highlight shared genetic risk across populations. *Nat Genet* 2015;47:979–986.
3. Kelsen J, Baldassano RN. Inflammatory bowel disease: the difference between children and adults. *Inflamm Bowel Dis* 2008;14(suppl 2):S9–S11.
4. Jostins L, Ripke S, Weersma RK, et al. Host-microbe interactions have shaped the genetic architecture of inflammatory bowel disease. *Nature* 2012;491:119–124.
5. de Lange KM, Moutsianas L, Lee JC, et al. Genome-wide association study implicates immune activation of multiple integrin genes in inflammatory bowel disease. *Nat Genet* 2017;49:256–261.
6. Molodecky NA, Soon IS, Rabi DM, et al. Increasing incidence and prevalence of the inflammatory bowel diseases with time, based on systematic review. *Gastroenterology* 2012;142:46–54.e42; quiz e30.
7. Benchimol EI, Fortinsky KJ, Gozdyra P, et al. Epidemiology of pediatric inflammatory bowel disease: a systematic review of international trends. *Inflamm Bowel Dis* 2011;17:423–439.
8. Virta LJ, Saarinen MM, Kolho KL. Inflammatory bowel disease incidence is on the continuous rise among all paediatric patients except for the very young: a nationwide registry-based study on 28-year follow-up. *J Crohns Colitis* 2017;11:150–156.
9. Haberman Y, Tickle TL, Dexheimer PJ, et al. Pediatric Crohn disease patients exhibit specific ileal transcriptome and microbiome signature. *J Clin Invest* 2014;124:3617–3633.
10. Häsler R, Sheibani-Tezerji R, Sinha A, et al. Uncoupling of mucosal gene regulation, mRNA splicing and adherent microbiota signatures in inflammatory bowel disease. *Gut* 2017;66:2087–2097.
11. Sokol H, Leduq V, Aschard H, et al. Fungal microbiota dysbiosis in IBD. *Gut* 2017;66:1039–1048.
12. Gevers D, Kugathasan S, Denson LA, et al. The treatment-naïve microbiome in new-onset Crohn's disease. *Cell Host Microbe* 2014;15:382–392.
13. Feil R, Fraga MF. Epigenetics and the environment: emerging patterns and implications. *Nat Rev Genet* 2012;13:97–109.
14. Zilbauer M, Zellos A, Heuschkel R, et al. Epigenetics in paediatric gastroenterology, hepatology, and nutrition: present trends and future perspectives. *J Pediatr Gastroenterol Nutr* 2016;62:521–552.

- 1561 15. Hasler R, Feng Z, Backdahl L, et al. A functional methy- 1621
 1562 lome map of ulcerative colitis. *Genome Res* 2012; 1622
 1563 22:2130–2137. 1623
 1564 16. Kraiczy J, Nayak K, Ross A, et al. Assessing DNA 1624
 1565 methylation in the developing human intestinal epithe- 1625
 1566 lium: potential link to inflammatory bowel disease. 1626
 1567 *Mucosal Immunol* 2016;9:647–658. 1627
 1568 17. Roadmap Epigenomics Consortium, Kundaje A, 1628
 1569 Meuleman W, et al. Integrative analysis of 111 reference 1629
 1570 human epigenomes. *Nature* 2015;518:317–330. 1630
 1571 18. Chen L, Ge B, Casale FP, et al. Genetic drivers of 1631
 1572 epigenetic and transcriptional variation in human immune 1632
 1573 cells. *Cell* 2016;167:1398–1414.e24. 1633
 1574 19. Kaser A, Pasaniuc B. IBD genetics: focus on (dys) 1634
 1575 regulation in immune cells and the epithelium. *Gastro-* 1635
 1576 *enterology* 2014;146:896–899. 1636
 1577 20. Adolph TE, Niederreiter L, Blumberg RS, et al. Endo- 1637
 1578 plasmic reticulum stress and inflammation. *Dig Dis* 2012; 1638
 1579 30:341–346. 1639
 1580 21. Hosomi S, Kaser A, Blumberg RS. Role of endoplasmic 1640
 1581 reticulum stress and autophagy as interlinking pathways 1641
 1582 in the pathogenesis of inflammatory bowel disease. *Curr* 1642
 1583 *Opin Gastroenterol* 2015;31:81–88. 1643
 1584 22. Levine A, Koletzko S, Turner D, et al. ESPGHAN revised 1644
 1585 porto criteria for the diagnosis of inflammatory bowel 1645
 1586 disease in children and adolescents. *J Pediatr Gastro-* 1646
 1587 *enterol Nutr* 2014;58:795–806. 1647
 1588 23. Jenke AC, Postberg J, Raine T, et al. DNA methylation 1648
 1589 analysis in the intestinal epithelium-effect of cell separa- 1649
 1590 tion on gene expression and methylation profile. *PLoS* 1650
 1591 *One* 2013;8:e55636. 1651
 1592 24. Sato T, Stange DE, Ferrante M, et al. Long-term expan- 1652
 1593 sion of epithelial organoids from human colon, adenoma, 1653
 1594 adenocarcinoma, and Barrett's epithelium. *Gastroenter-* 1654
 1595 *ology* 2011;141:1762–1772. 1655
 1596 25. Aryee MJ, Jaffe AE, Corrada-Bravo H, et al. Minfi: a 1656
 1597 flexible and comprehensive Bioconductor package for 1657
 1598 the analysis of Infinium DNA methylation microarrays. 1658
 1599 *Bioinformatics* 2014;30:1363–1369. 1659
 1600 26. Leek JT, Johnson WE, Parker HS, et al. The sva package 1660
 1601 for removing batch effects and other unwanted variation 1661
 1602 in high-throughput experiments. *Bioinformatics* 2012; 1662
 1603 28:882–883. 1663
 1604 27. Peters TJ, Buckley MJ, Statham AL, et al. De novo 1664
 1605 identification of differentially methylated regions in the 1665
 1606 human genome. *Epigenetics Chromatin* 2015;8:6. 1666
 1607 28. Ritchie ME, Phipson B, Wu D, et al. limma powers dif- 1667
 1608 ferential expression analyses for RNA-sequencing and 1668
 1609 microarray studies. *Nucleic Acids Res* 2015;43:e47. 1669
 1610 29. McMurdie PJ, Holmes S. phyloseq: An R Package for 1670
 1611 reproducible interactive analysis and graphics of micro- 1671
 1612 biome census data. *PLoS One* 2013;8:e61217. 1672
 1613 30. Love MI, Huber W, Anders S. Moderated estimation of 1673
 1614 fold change and dispersion for RNA-seq data with 1674
 1615 DESeq2. *Genome Biol* 2014;15:550. 1675
 1616 31. Breuer K, Froushani AK, Laird MR, et al. InnateDB: 1676
 1617 systems biology of innate immunity and beyond—recent 1677
 1618 updates and continuing curation. *Nucleic Acids Res* 1678
 1619 2013;41:D1228–D1233. 1679
 1620 32. Langfelder P, Horvath S. WGCNA: an R package for 1680
 1621 weighted correlation network analysis. *BMC Bioinforma-* 1681
 1622 *tics* 2008;9:559. 1682
 1623 33. Becker C, Watson AJ, Neurath MF. Complex roles of 1683
 1624 caspases in the pathogenesis of inflammatory bowel 1684
 1625 disease. *Gastroenterology* 2013;144:283–293. 1685
 1626 34. Hershberg RM, Mayer LF. Antigen processing and pre- 1686
 1627 sentation by intestinal epithelial cells - polarity and 1687
 1628 complexity. *Immunol Today* 2000;21:123–128. 1688
 1629 35. Dotti I, Mora-Buch R, Ferrer-Picon E, et al. Alterations in 1689
 1630 the epithelial stem cell compartment could contribute to 1690
 1631 permanent changes in the mucosa of patients with 1691
 1632 ulcerative colitis. *Gut* 2017;66:2069–2079. 1692
 1633 36. Peloquin JM, Goel G, Kong L, et al. Characterization of 1693
 1634 candidate genes in inflammatory bowel disease- 1694
 1635 associated risk loci. *JCI Insight* 2016;1:e87899. 1695
 1636 37. Peters JE, Lyons PA, Lee JC, et al. Insight into genotype- 1696
 1637 phenotype associations through eQTL mapping in 1697
 1638 multiple cell types in health and immune-mediated 1698
 1639 disease. *PLoS Genet* 2016;12:e1005908. 1699
 1640 38. Meddens CA, Harakalova M, van den Dungen NA, et al. 1700
 1641 Systematic analysis of chromatin interactions at disease 1701
 1642 associated loci links novel candidate genes to inflam- 1702
 1643 matory bowel disease. *Genome Biol* 2016;17:247. 1703
 1644 39. Ventham NT, Kennedy NA, Adams AT, et al. Integrative 1704
 1645 epigenome-wide analysis demonstrates that DNA 1705
 1646 methylation may mediate genetic risk in inflammatory 1706
 1647 bowel disease. *Nat Commun* 2016;7:13507. 1707
 1648 40. McKinney EF, Lee JC, Jayne DR, et al. T-cell exhaustion, 1708
 1649 co-stimulation and clinical outcome in autoimmunity and 1709
 1650 infection. *Nature* 2015;523:612–616. 1710
 1651 41. Tauschmann M, Prietl B, Treiber G, et al. Distribution of 1711
 1652 CD4(pos) -, CD8(pos) - and regulatory T cells in the upper 1712
 1653 and lower gastrointestinal tract in healthy young sub- 1713
 1654 jects. *PLoS One* 2013;8:e80362. 1714
 1655 1715
 1656 1716
 1657 1717
 1658 1718
 1659 1719
 1660 1720
 1661 1721
 1662 1722
 1663 1723
 1664 1724
 1665 1725
 1666 1726
 1667 1727
 1668 1728
 1669 1729
 1670 1730
 1671 1731
 1672 1732
 1673 1733
 1674 1734
 1675 1735
 1676 1736
 1677 1737
 1678 1738
 1679 1739
 1680 1740
 1681 1741
 1682 1742
 1683 1743
 1684 1744
 1685 1745
 1686 1746
 1687 1747
 1688 1748
 1689 1749
 1690 1750
 1691 1751
 1692 1752
 1693 1753
 1694 1754
 1695 1755
 1696 1756
 1697 1757
 1698 1758
 1699 1759
 1700 1760
 1701 1761
 1702 1762
 1703 1763
 1704 1764
 1705 1765
 1706 1766
 1707 1767
 1708 1768
 1709 1769
 1710 1770
 1711 1771
 1712 1772
 1713 1773
 1714 1774
 1715 1775
 1716 1776
 1717 1777
 1718 1778
 1719 1779
 1720 1780
 1721 1781
 1722 1782
 1723 1783
 1724 1784
 1725 1785
 1726 1786
 1727 1787
 1728 1788
 1729 1789
 1730 1790
 1731 1791
 1732 1792
 1733 1793
 1734 1794
 1735 1795
 1736 1796
 1737 1797
 1738 1798
 1739 1799
 1740 1800
 1741 1801
 1742 1802
 1743 1803
 1744 1804
 1745 1805
 1746 1806
 1747 1807
 1748 1808
 1749 1809
 1750 1810
 1751 1811
 1752 1812
 1753 1813
 1754 1814
 1755 1815
 1756 1816
 1757 1817
 1758 1818
 1759 1819
 1760 1820
 1761 1821
 1762 1822
 1763 1823
 1764 1824
 1765 1825
 1766 1826
 1767 1827
 1768 1828
 1769 1829
 1770 1830
 1771 1831
 1772 1832
 1773 1833
 1774 1834
 1775 1835
 1776 1836
 1777 1837
 1778 1838
 1779 1839
 1780 1840
 1781 1841
 1782 1842
 1783 1843
 1784 1844
 1785 1845
 1786 1846
 1787 1847
 1788 1848
 1789 1849
 1790 1850
 1791 1851
 1792 1852
 1793 1853
 1794 1854
 1795 1855
 1796 1856
 1797 1857
 1798 1858
 1799 1859
 1800 1860
 1801 1861
 1802 1862
 1803 1863
 1804 1864
 1805 1865
 1806 1866
 1807 1867
 1808 1868
 1809 1869
 1810 1870
 1811 1871
 1812 1872
 1813 1873
 1814 1874
 1815 1875
 1816 1876
 1817 1877
 1818 1878
 1819 1879
 1820 1880
 1821 1881
 1822 1882
 1823 1883
 1824 1884
 1825 1885
 1826 1886
 1827 1887
 1828 1888
 1829 1889
 1830 1890
 1831 1891
 1832 1892
 1833 1893
 1834 1894
 1835 1895
 1836 1896
 1837 1897
 1838 1898
 1839 1899
 1840 1900
 1841 1901
 1842 1902
 1843 1903
 1844 1904
 1845 1905
 1846 1906
 1847 1907
 1848 1908
 1849 1909
 1850 1910
 1851 1911
 1852 1912
 1853 1913
 1854 1914
 1855 1915
 1856 1916
 1857 1917
 1858 1918
 1859 1919
 1860 1920
 1861 1921
 1862 1922
 1863 1923
 1864 1924
 1865 1925
 1866 1926
 1867 1927
 1868 1928
 1869 1929
 1870 1930
 1871 1931
 1872 1932
 1873 1933
 1874 1934
 1875 1935
 1876 1936
 1877 1937
 1878 1938
 1879 1939
 1880 1940
 1881 1941
 1882 1942
 1883 1943
 1884 1944
 1885 1945
 1886 1946
 1887 1947
 1888 1948
 1889 1949
 1890 1950
 1891 1951
 1892 1952
 1893 1953
 1894 1954
 1895 1955
 1896 1956
 1897 1957
 1898 1958
 1899 1959
 1900 1960
 1901 1961
 1902 1962
 1903 1963
 1904 1964
 1905 1965
 1906 1966
 1907 1967
 1908 1968
 1909 1969
 1910 1970
 1911 1971
 1912 1972
 1913 1973
 1914 1974
 1915 1975
 1916 1976
 1917 1977
 1918 1978
 1919 1979
 1920 1980
 1921 1981
 1922 1982
 1923 1983
 1924 1984
 1925 1985
 1926 1986
 1927 1987
 1928 1988
 1929 1989
 1930 1990
 1931 1991
 1932 1992
 1933 1993
 1934 1994
 1935 1995
 1936 1996
 1937 1997
 1938 1998
 1939 1999
 1940 2000
 1941 2001
 1942 2002
 1943 2003
 1944 2004
 1945 2005
 1946 2006
 1947 2007
 1948 2008
 1949 2009
 1950 2010
 1951 2011
 1952 2012
 1953 2013
 1954 2014
 1955 2015
 1956 2016
 1957 2017
 1958 2018
 1959 2019
 1960 2020
 1961 2021
 1962 2022
 1963 2023
 1964 2024
 1965 2025
 1966 2026
 1967 2027
 1968 2028
 1969 2029
 1970 2030
 1971 2031
 1972 2032
 1973 2033
 1974 2034
 1975 2035
 1976 2036
 1977 2037
 1978 2038
 1979 2039
 1980 2040
 1981 2041
 1982 2042
 1983 2043
 1984 2044
 1985 2045
 1986 2046
 1987 2047
 1988 2048
 1989 2049
 1990 2050
 1991 2051
 1992 2052
 1993 2053
 1994 2054
 1995 2055
 1996 2056
 1997 2057
 1998 2058
 1999 2059
 2000 2060
 2001 2061
 2002 2062
 2003 2063
 2004 2064
 2005 2065
 2006 2066
 2007 2067
 2008 2068
 2009 2069
 2010 2070
 2011 2071
 2012 2072
 2013 2073
 2014 2074
 2015 2075
 2016 2076
 2017 2077
 2018 2078
 2019 2079
 2020 2080
 2021 2081
 2022 2082
 2023 2083
 2024 2084
 2025 2085
 2026 2086
 2027 2087
 2028 2088
 2029 2089
 2030 2090
 2031 2091
 2032 2092
 2033 2093
 2034 2094
 2035 2095
 2036 2096
 2037 2097
 2038 2098
 2039 2099
 2040 2100
 2041 2101
 2042 2102
 2043 2103
 2044 2104
 2045 2105
 2046 2106
 2047 2107
 2048 2108
 2049 2109
 2050 2110
 2051 2111
 2052 2112
 2053 2113
 2054 2114
 2055 2115
 2056 2116
 2057 2117
 2058 2118
 2059 2119
 2060 2120
 2061 2121
 2062 2122
 2063 2123
 2064 2124
 2065 2125
 2066 2126
 2067 2127
 2068 2128
 2069 2129
 2070 2130
 2071 2131
 2072 2132
 2073 2133
 2074 2134
 2075 2135
 2076 2136
 2077 2137
 2078 2138
 2079 2139
 2080 2140
 2081 2141
 2082 2142
 2083 2143
 2084 2144
 2085 2145
 2086 2146
 2087 2147
 2088 2148
 2089 2149
 2090 2150
 2091 2151
 2092 2152
 2093 2153
 2094 2154
 2095 2155
 2096 2156
 2097 2157
 2098 2158
 2099 2159
 2100 2160
 2101 2161
 2102 2162
 2103 2163
 2104 2164
 2105 2165
 2106 2166
 2107 2167
 2108 2168
 2109 2169
 2110 2170
 2111 2171
 2112 2172
 2113 2173
 2114 2174
 2115 2175
 2116 2176
 2117 2177
 2118 2178
 2119 2179
 2120 2180
 2121 2181
 2122 2182
 2123 2183
 2124 2184
 2125 2185
 2126 2186
 2127 2187
 2128 2188
 2129 2189
 2130 2190
 2131 2191
 2132 2192
 2133 2193
 2134 2194
 2135 2195
 2136 2196
 2137 2197
 2138 2198
 2139 2199
 2140 2200
 2141 2201
 2142 2202
 2143 2203
 2144 2204
 2145 2205
 2146 2206
 2147 2207
 2148 2208
 2149 2209
 2150 2210
 2151 2211
 2152 2212
 2153 2213
 2154 2214
 2155 2215
 2156 2216
 2157 2217
 2158 2218
 2159 2219
 2160 2220
 2161 2221
 2162 2222
 2163 2223
 2164 2224
 2165 2225
 2166 2226
 2167 2227
 2168 2228
 2169 2229
 2170 2230
 2171 2231
 2172 2232
 2173 2233
 2174 2234
 2175 2235
 2176 2236
 2177 2237
 2178 2238
 2179 2239
 2180 2240
 2181 2241
 2182 2242
 2183 2243
 2184 2244
 2185 2245
 2186 2246
 2187 2247
 2188 2248
 2189 2249
 2190 2250
 2191 2251
 2192 2252
 2193 2253
 2194 2254
 2195 2255
 2196 2256
 2197 2257
 2198 2258
 2199 2259
 2200 2260
 2201 2261
 2202 2262
 2203 2263
 2204 2264
 2205 2265
 2206 2266
 2207 2267
 2208 2268
 2209 2269
 2210 2270
 2211 2271
 2212 2272
 2213 2273
 2214 2274
 2215 2275
 2216 2276
 2217 2277
 2218 2278
 2219 2279
 2220 2280
 2221 2281
 2222 2282
 2223 2283
 2224 2284
 2225 2285
 2226 2286
 2227 2287
 2228 2288
 2229 2289
 2230 2290
 2231 2291
 2232 2292
 2233 2293
 2234 2294
 2235 2295
 2236 2296
 2237 2297
 2238 2298
 2239 2299
 2240 2300
 2241 2301
 2242 2302
 2243 2303
 2244 2304
 2245 2305
 2246 2306
 2247 2307
 2248 2308
 2249 2309
 2250 2310
 2251 2311
 2252 2312
 2253 2313
 2254 2314
 2255 2315
 2256 2316
 2257 2317
 2258 2318
 2259 2319
 2260 2320
 2261 2321
 2262 2322
 2263 2323
 2264 2324
 2265 2325
 2266 2326
 2267 2327
 2268 2328
 2269 2329
 2270 2330
 2271 2331
 2272 2332
 2273 2333
 2274 2334
 2275 2335
 2276 2336
 2277 2337
 2278 2338
 2279 2339
 2280 2340
 2281 2341
 2282 2342
 2283 2343
 2284 2344
 2285 2345
 2286 2346
 2287 2347
 2288 2348
 2289 2349
 2290 2350
 2291 2351
 2292 2352
 2293 2353
 2294 2354
 2295 2355
 2296 2356
 2297 2357
 2298 2358
 2299 2359
 2300 2360
 2301 2361
 2302 2362
 2303 2363
 2304 2364
 2305 2365
 2306 2366
 2307 2367
 2308 2368
 2309 2369
 2310 2370
 23